AJNR

Aqueductal blood clot as a cause of acute hydrocephalus in subarachnoid hemorrhage.

Y Yoshimoto, C Ochiai, K Kawamata, M Endo and M Nagai

AJNR Am J Neuroradiol 1996, 17 (6) 1183-1186
http://www.ajnr.org/content/17/6/1183

Aqueductal Blood Clot as a Cause of Acute Hydrocephalus in Subarachnoid Hemorrhage

Yuhei Yoshimoto, Chikayuki Ochiai, Kazumi Kawamata, Masaru Endo, and Masakatsu Nagai

Summary: We describe two patients with acute hydrocephalus, in whom CT scans did not show intraventricular hemorrhage unequivocally. Midline sagittal MR imaging revealed a blood clot plugging the aqueduct. MR imaging is useful for detecting subacute clots within the aqueduct and for differentiating them from other entities.

Index terms: Aqueduct of Sylvius; Hydrocephalus; Subarachnoid space, hemorrhage

The aqueduct is the most common site of intraventricular blockade of the flow of cerebrospinal fluid (CSF), evidently because it is the narrowest passage (1). Radiologic investigations, including ventriculography, pneumoencephalography, and computed tomography (CT) frequently fail to show various entities such as congenital anomalies, tumors, and cysts in this region (2, 3). Magnetic resonance (MR) imaging of patients with unexplained aqueductal stenosis or occlusion has shown such lesions to be the cause of hydrocephalus (2–5). Recently, we encountered two patients with acute hydrocephalus caused by intraventricular small clots plugging the aqueduct. MR images showed these lesions in both cases.

Case Reports

Case 1

A 50-year-old man with hypertension was admitted with progressively declining consciousness and a 1-week history of headache. He was semicomatose with moderate neck stiffness, but no motor paresis. His pupils were small and reacted sluggishly to light. CT scans showed a small, faint, high-density area in the head of the left caudate nucleus, dilatation of the lateral and third ventricles, and a normal fourth ventricle (Fig 1A). No intraventricular hemorrhage was evident.

Immediate ventriculostomy improved his neurologic condition. MR imaging, performed 4 days after admission, defined a small clot in the posterior part of the third ventricle plugging the aqueduct (Fig 1B). This clot was hyperintense on T1-weighted images and hypointense on T2-weighted images. The postcontrast T1-weighted image showed no abnormal enhancement.

Cerebral angiography revealed no vascular anomaly, and the cause of the intracerebral hematoma in the head of the caudate nucleus, which presumably occurred 1 week before admission, was thought to be hypertension. Subsequent MR imaging, performed 18 days after admission, showed that the lesion had disappeared (Fig 1C). Twenty-two days after admission the patient was discharged from the hospital with no neurologic deficit.

Case 2

A 59-year-old man was admitted with progressively declining consciousness. Owing to mental retardation from childhood, he had lived in a protective institute, although he had been independent in his daily life. On admission, he was stuporous but withdrew his extremities in response to painful stimuli. His pupils were miotic, but reacted promptly to light. A CT scan showed dilated lateral and third ventricles, but a normal fourth ventricle, cortical atrophy, and no intracranial hemorrhage (Fig 2A). Sagittal T1-weighted MR imaging, performed on the day of admission, showed a hyperintense plug in the aqueduct (Fig 2B); the postcontrast T1-weighted image showed no abnormal enhancement. The lesion appeared hypointense on T2-weighted images and was thought to be a subacute blood clot. Angiography revealed complete occlusion of both internal carotid arteries and collateral flow via the external carotid artery, which was diagnosed as moyamoya disease, to which his mental retardation could be attributed. Ventriculostomy was carried out immediately, and he gradually recovered to his previous state. Follow-up MR imaging performed 17 days later showed that the blood clot had disappeared completely (Fig 2C).

Received June 28, 1995; accepted after revision October 5.

From the Department of Neurosurgery, Dokkyo University School of Medicine, Tochigi, Japan.

Address reprint requests to Yuhei Yoshimoto, MD, Department of Neurosurgery, Dokkyo University School of Medicine, 880 Kitakobayashi, Mibu, Shimotsuga, Tochigi 321-02, Japan.

AJNR 17:1183–1186, Jun 1996 0195-6108/96/1706–1183

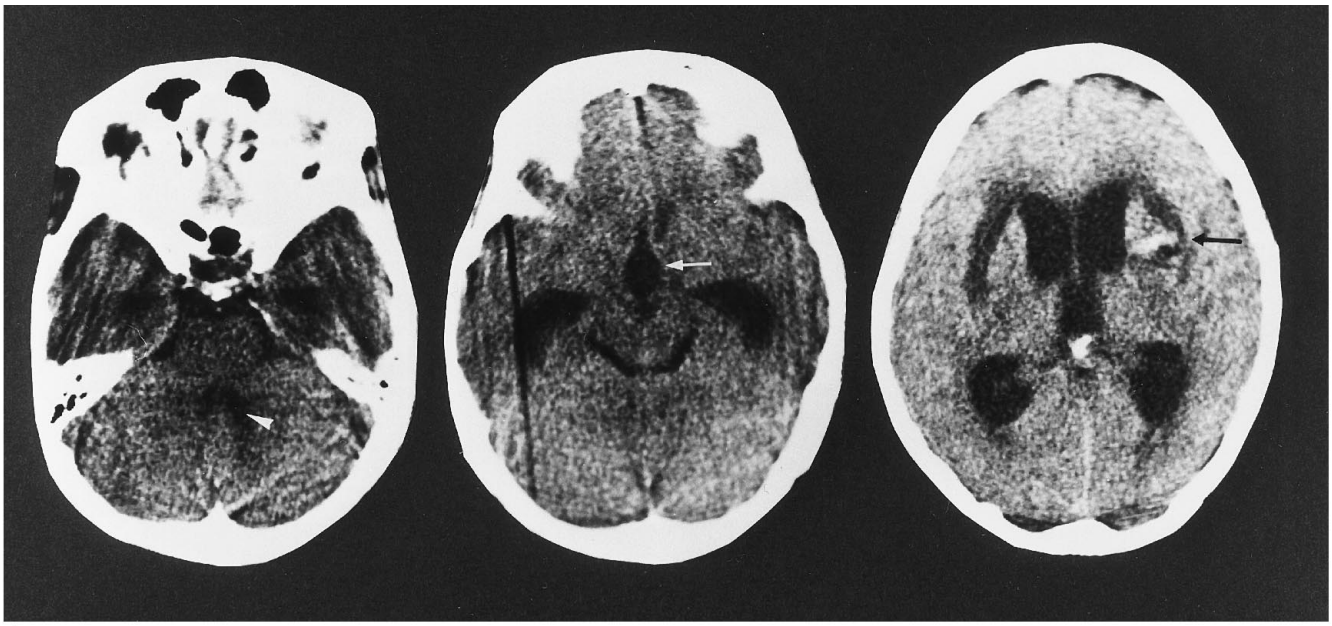

A

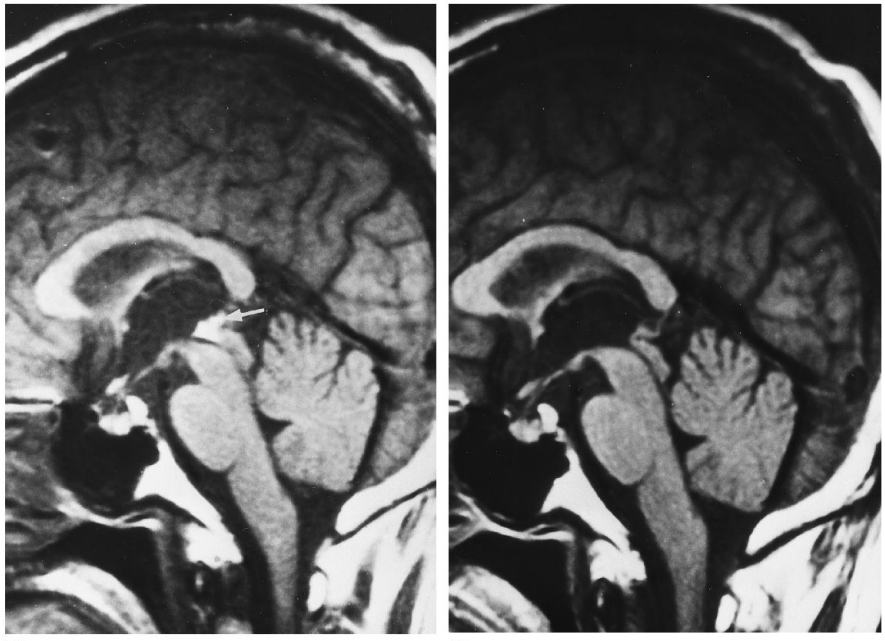

B C

Fig 1. Case 1.

A, CT scans show a small, faint, high-density area in the head of the left caudate nucleus (*black arrow*) and dilatation of the lateral and third ventricles (*white arrow*). The size of the fourth ventricle is normal (*arrowhead*). No intraventricular hemorrhage is evident.

B, T1-weighted sagittal MR image (500/20 [repetition time/echo time]) obtained 4 days after admission shows a high-intensity mass (*arrow*) in the posterior part of the third ventricle plugging the upper portion of the aqueduct.

C, MR image obtained 18 days after admission shows that the lesion has disappeared completely.

Discussion

Obstruction of the aqueduct of Sylvius is a well-recognized condition that results from congenital or acquired lesions. The aqueduct functions as a conduit for the passage of CSF between the third and fourth ventricles, and is a point of marked narrowing with a long course in the CSF pathway. In fixed brain specimens, the aqueduct forms a gentle curve in the upper portion and has two areas of relative constriction: one at the level of the superior colliculus and the other at the level of the intercollicular sulcus. These divide the aqueduct into a pars anterior, an ampulla, and a pars posterior (1). In cross section, the aqueductal lumen is triangular at the area of constriction and ovoid at the ampulla. The cross-sectional area of the narrowest segment varies widely among individuals (mean, 0.9; range, 0.2 to 1.8 mm^2) (1). The length of the aqueduct is reported to vary in-

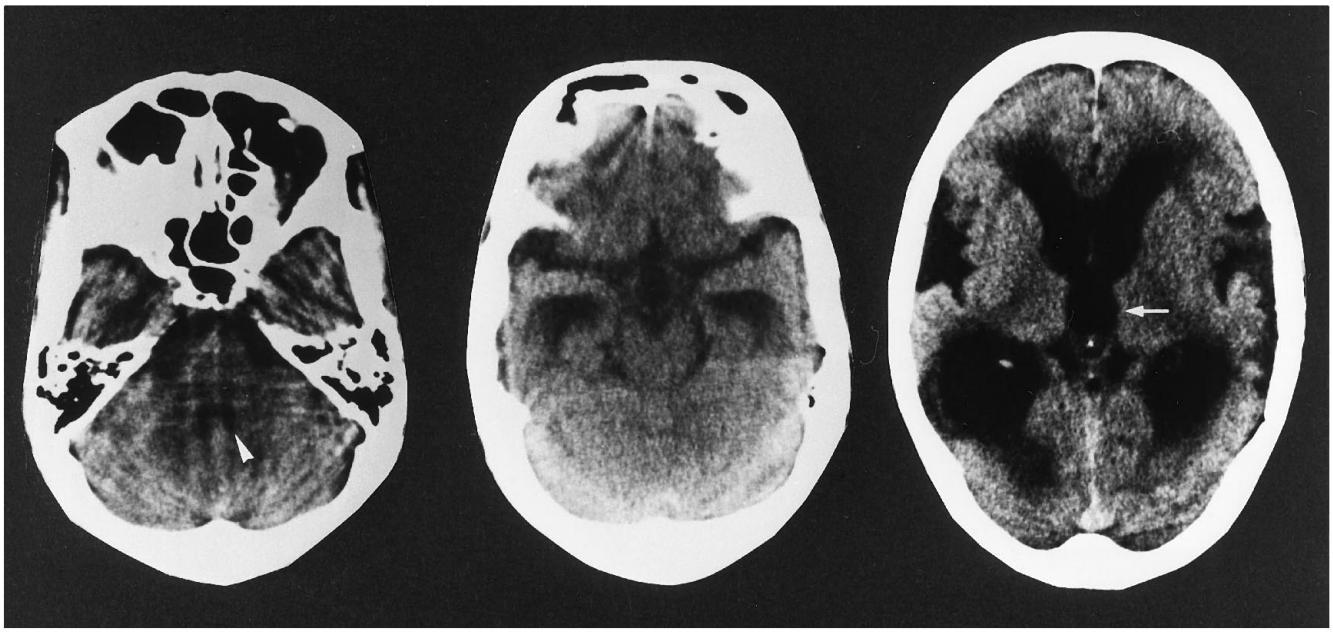

A

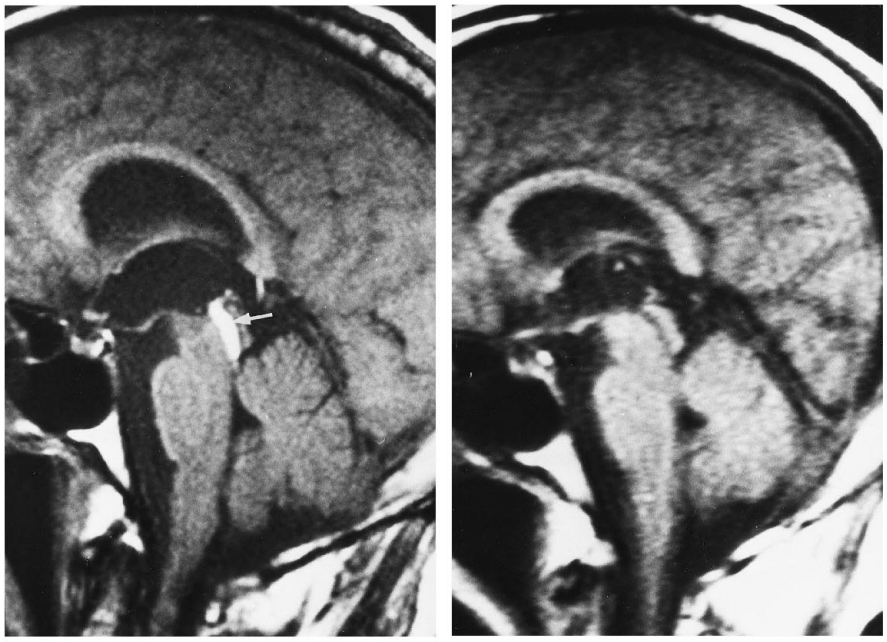

B C

Fig 2. Case 2.

A, CT scans show marked dilatation of the lateral and third ventricles (*arrow*) and a normal fourth ventricle (*arrowhead*). However, no intracranial hemorrhage is seen at any section level.

B, Sagittal T1-weighted MR image (300/15) shows a small hyperintense lesion (*arrow*) plugging the aqueduct.

C, Follow-up MR image obtained 17 days later shows that the mass has disappeared completely.

versely according to its mean cross-sectional area so that longer aqueducts tend to be those with smaller mean cross-sectional areas (1), probably because of stretching of the aqueduct (6), and vice versa. A long, narrow aqueduct may be susceptible to blockade of CSF flow, which is likely to lead to obstructive hydrocephalus. It is possible that obstruction sufficient to produce hydrocephalus in one brain will fail to do so in another.

Intraventricular hemorrhage is frequently accompanied by acute hydrocephalus. In such cases, the hematoma is usually voluminous and evident on CT scans. In our two patients, the blood clots within the ventricles were so small that the CT scans failed to show them. The ventricular dilatation patterns (enlarged lateral and third ventricles but normal fourth ventricle) strongly suggested the presence of periaqueductal lesions, prompting us to perform MR im-

aging. The midline sagittal sections shown on T1-weighted images revealed blood clot within the aqueduct, although the exact locations of the clots in the two patients differed somewhat: capping of the aqueductal entrance in case 1, and complete plugging throughout the aqueduct in case 2. In both cases, the lesions were hyperintense on T1-weighted images and hypointense on T2-weighted images. Such an appearance is compatible with subacute hematoma (7, 8), which can be differentiated easily from other entities. Contrast-enhanced T1-weighted images were useful to rule out periaqueductal tumor. The causes of the intraventricular hemorrhages were considered to be slight leakage from an intracerebral hemorrhage due to hypertension in case 1 and minor bleeding from subependymal abnormal vessels due to moyamoya disease in case 2. Subsequent MR imaging showed that the blood clots within the aqueducts of both patients disappeared completely within 17 to 18 days. Therefore, temporary ventriculostomy, as performed in our patients, seems to be appropriate treatment for such patients.

The findings in our patients indicate that even a minimal intraventricular blood clot can cause acute hydrocephalus as a result of aqueductal obstruction. Primary midbrain hemorrhages and vascular anomalies have been verified by MR imaging to cause aqueductal obstruction (4, 5, 9). As CT missed the small clots in our patients, it is likely that diagnoses were not accurate in a number of such patients in the past. Multiplanar MR imaging is useful for the diagnosis of periaqueductal lesions, especially in this phase of hemorrhage.

Although MR imaging may be misleading on days 1 through 3, since the clot will generally be isointense with brain on T1-weighted images and only slightly hypointense on T2-weighted images, extracellular methemoglobin becomes bright on T1-weighted images obtained after day 4 or 5 (7, 10). Augustyn et al (11) described a patient with a fresh thrombus in the aperture of the aqueduct related to a large giant-cell astrocytoma, which could have been misinterpreted as indicating aqueductal patency because of absence of signal on T2-weighted images. However, a T1-weighted image, which was not obtained in their patient, might have distinguished it from a CSF flow void, providing enough time had elapsed for cell membrane lysis and methemoglobin formation to occur.

In the acute setting, CT is useful for the diagnosis of intraventricular hemorrhage. We think that both CT and MR imaging are necessary for accurate diagnosis. MR imaging delineates the fine internal architecture in the vicinity of the aqueduct and enables CSF flow to be assessed (flow-related signal void) (5). The direct multiplanar imaging capability of MR, particularly in the sagittal plane, makes this technique more useful than previously used methods. Defining the morphology and any disease-induced distortions of the aqueduct of Sylvius will help to determine the correct management of patients with hydrocephalus.

References

1. Woolom DHM, Millen JW. Anatomical considerations in the pathology of stenosis of the cerebral aqueduct. *Brain* 1953;76:104–112
2. Boydston WR, Sanford RA, Muhlbauer MS, et al. Gliomas of the tectum and periaqueductal region of the mesencephalon. *Pediatr Neurosurg* 1991;17:234–238
3. Lee BCP. Magnetic resonance imaging of peri-aqueductal lesions. *Clin Radiol* 1987;38:527–533
4. Friedman DP. Extrapineal abnormality of the tectal region: MR imaging findings. *AJR Am J Roentgenol* 1992;159:859–866
5. Kemp SS, Zimmerman RA, Bilaniuk LT, Hackney DB, Goldberg HI, Grossman RI. Magnetic resonance imaging of the cerebral aqueduct. *Neuroradiology* 1987;29:430–436
6. Lichtenstein BW. Distant neuroanatomic complications of spina bifida (spinal dysraphism): Hydrocephalus, Arnold-Chiari deformity, stenosis of the aqueduct of Sylvius, etc: pathogenesis and pathology. *Arch Neurol Psychiat* 1942;47:195–214
7. Gomori JM, Grossman RI, Hackney DB, Goldberg HI, Zimmerman RA, Bilaniuk LT. Variable appearances of subacute intracranial hematomas on high-field spin-echo MR. *AJNR Am J Neuroradiol* 1987;8:1019–1026
8. Sipponen JT, Sipponen RE, Sivula A. Nuclear magnetic resonance (NMR) imaging of intracerebral hemorrhage in the acute and resolving phases. *J Comput Assist Tomogr* 1983;7:954–959
9. Sand JJ, Biller JB, Corbett JJ, Adams HP, Dunn V. Partial dorsal mesencephalic hemorrhage: report of three cases. *Neurology* 1986;36:529–533
10. Bradley WG, Schmidt PG. Effect of methemoglobin formation on the MR appearance of subarachnoid hemorrhage. *Radiology* 1985;156:99–103
11. Augustyn GT, D'Amour PG, Scott JA, Worth RM. Thrombus simulating flow void: a pitfall in diagnosing aqueductal patency by high-field MR imaging. *AJNR Am J Neuroradiol* 1987;8:1139–1141